Quantum theory of intersubband polarons

Simone De Liberato, Cristiano Ciuti

Quantum theory of intersubband polarons

Simone De Liberato and Cristiano Ciuti

Laboratoire Matériaux et Phénomènes Quantiques,
Université Paris Diderot-Paris 7 and CNRS, UMR 7162, 75013 Paris, France

We present a microscopic quantum theory of intersubband polarons, quasiparticles originated from the coupling between intersubband transitions and longitudinal optical phonons. To this aim we develop a second quantized theory taking into account the Fröhlich interaction between phonons and intersubband transitions and the Coulomb interaction between the intersubband transitions themselves. Our results show that the coupling between the phonons and the intersubband transitions is extremely intense, thanks both to the collective nature of the intersubband excitation and to the natural tight confinement of optical phonons. Not only the coupling is strong enough to spectroscopically resolve the resonant splitting between the modes (strong coupling regime), but it can become comparable to the bare frequency of the excitations (ultrastrong coupling regime). We thus predict the possibility to exploit intersubband polarons both for applied optoelectronic research, where a precise control of the phonon resonances is needed, and also to observe fundamental quantum vacuum physics, typical of the ultrastrong coupling regime.

I. INTRODUCTION

The theory of polarons, the quasiparticles describing electrons moving in a polarizable medium, dates back to the early days of quantum theory[1], and it has been an active field of research ever since[2]. Polarons have been studied both for three[3] and two[4,5] dimensional electron gases, leading to a number of very precise estimates of the quasiparticle mass and energy.

In this paper we will talk of strongly and ultrastrongly coupled polarons. In polaron theory it is customary to distinguish between weak coupling[6] and strong coupling[7] polarons, accordingly to the value of the Fröhlich coupling constant, that quantifies the strength of the electron-phonon coupling, and that is used as development parameter in perturbative calculations[8]. In this paper anyway we will use the terms *strong* and *ultrastrong* coupling in a different, even if closely related, meaning.

The term strong coupling is commonly used in modern atomic and solid state physics with a rather precise meaning: two systems are strongly coupled if it is possible to resolve, at resonance, the anticrossing due to the coupling. Strong coupling in this latter sense has been predicted[9,10] and observed[11,12] very early for polaritons coupled to three dimensional plasmons.

The figure of merit of the strong coupling regime is the ratio between the coupling strength, quantified by the so-called vacuum Rabi frequency Ω, and the width of the resonance Γ. If $\frac{\Omega}{\Gamma}$ is bigger than one, the two resonances are spectroscopically resolved, and the system is in the strong coupling regime. An interesting point to be made is that the fact of whether a system is in the strong coupling regime or not, does not depend on the intrinsic strength of the coupling, but only on the ratio between the coupling and the linewidth; the first observations of the strong coupling regime in atomic systems were made with Rydberg atoms in superconducting cavities, where the strength of the coupling is negligible when compared to the bare frequency of the involved transitions ω, but

where the astounding quality factor of the superconducting cavities allows to resolve the resonant splitting[13].

It is easy to prove that the value of the ratio $\frac{\Omega}{\omega}$ for atomic systems is always much smaller than one, its smallness being linked with the value of the fine structure constant[14]. Still this severe limitation is valid only for single particle effects, while collective excitations can beat it thanks to their coherent nature. In a phenomenon reminiscent of the Dicke superradiance[15], the strength of the coupling scales as the square root of the number of particles involved, leading to the possibility to obtain values of $\frac{\Omega}{\omega}$ of the order of one.

This observation has prompted the development of the theory of the so-called ultrastrong coupling regime, that is the regime in which the coupling between two systems is of the same order of their bare frequencies. Such theory was initially developed[16,17] in the case of intersubband polaritons[18] in semiconductor quantum wells, where it was also observed for the first time[19–21]. The ultrastrong coupling regime has since been studied in a lot of different systems, ranging from circuit quantum electrodynamics[22,23], to organic semiconductors[24], to high mobility electron gases in presence of a perpendicular magnetic field[25,26].

The interest in such ultrastrong coupling regime is motivated by a whole range of new physics that can be observed: from spectral deformations[20], to quantum vacuum emission phenomena[27–29] and even quantum phase transitions[30,31].

This started a race to get the system with the highest value of the light-matter coupling ratio $\frac{\Omega}{\omega}$, with actual record values of 0.12 in superconducting circuits[23], 0.16 in organic molecules[24], 0.24 in semiconductor quantum wells[21] and 0.36 for two dimensional electron gases in presence of an applied magnetic field[26] (all coupled to a confined electromagnetic field).

It is natural at this point to ask how strong the coupling of polarons really is. It turns out that, in the case of coupling to collective excitations, it is quite big. Already for the first observation of three dimensional

plasmon-polaritons[11,12] we have $\frac{\Omega}{\omega} \simeq 0.2$ and values only marginally smaller were observed for polarons in quantum dots[32,33].

In this paper we will develop a microscopic theory of the ultrastrong coupling between intersubband transitions and longitudinal optical (LO) phonons in semiconductor quantum wells, that is the theory of ultrastrongly coupled intersubband polarons. The coupling between intersubband transitions and LO-phonons is relevant for a number of optoelectronic applications, as it determines the lifetime of carriers in excited subbands[34]. In particular a precise knowledge of LO-phonons intersubband scattering rates is important in the engineering of heterostructures for quantum cascade lasers[35]. Normally optoelectronic devices are designed to avoid being in resonance with optical phonon transitions, due to the high absorption between transverse and longitudinal optical phonon frequencies (Restrahlen band). A notable exception is provided by quantum cascade lasers operating near such optical resonances[36,37] in which instead the transitions between different subbands are almost resonant with LO-phonon modes.

Even if the coupling between intersubband transitions and LO-phonons in semiconductor quantum wells has indeed received some attention[38–40] and intersubband polaron resonances have been clearly and unambiguously observed[41], the fact that such mixed excitations can be extremely easily in the strong (or even ultrastrong) coupling regime seems overlooked by the community working on intersubband optoelectronic devices. Moreover, to the best of our knowledge, there is no microscopic theory of such excitations, as the spectra of intersubband polarons are normally calculated in an indirect way.

In the Sec. II we explain how our microscopic theory differs from the dielectric function approach normally employed to calculate the spectra of intersubband polarons. In order to build such microscopic theory, we will need to develop an exactly solvable Hamiltonian theory of electron-phonon and electron-electron interactions, heavily relying on the concept of superradiant, or coherent, excitation. In Sec. III, we will explain the general concept of superradiant excitations, that will then be extensively used in Sec. IV to construct the actual theory. In Sec. V we will apply the theory to the case of GaAs quantum wells, showing how the ultrastrong coupling regime can be reached even with such relatively weakly polar material. Finally a few considerations on the impact of our results and on possible future developments will be drawn in Sec. VI.

II. LONGITUDINAL EXCITATIONS

Electromagnetism in condensed matter physics is usually studied in the Coulomb gauge. This gauge, while not adapted to high energy physics due to its non-manifestly-covariant form, is particularly well suited to study low energy phenomena, thanks to a natural separation of dynamical and instantaneous degrees of freedom. In such gauge we have that, in absence of charges,

$$\text{div}[E(\omega)] = 0, \tag{1}$$

i.e., all propagating waves are transverse. When we consider the propagation of an electromagnetic wave in a dispersive medium, Eq. (1) becomes

$$\text{div}[D(\omega)] = \text{div}[\epsilon(\omega)E(\omega)] = 0, \tag{2}$$

that is, in a dispersive medium, it is possible to have propagating longitudinal waves at the frequencies for which

$$\Re[\epsilon(\omega)] = 0, \tag{3}$$

where $\Re$ indicates the real part. In order to find the frequencies of longitudinal modes it is thus customary to solve Eq. (3) for ω.

If we consider light propagating in a polar material, we can write the equation of the electromagnetic field coupled to the transverse optical (TO) phonons and from there we can calculate the dielectric function and finally use it in Eq. (3) to find the frequency of the LO-phonons. An interesting consequence of this approach is that we are calculating the frequency of the LO-phonon mode, considering the coupling of two fields that are not even coupled to it, as the propagating electromagnetic field couples to the TO-phonons, not to the LO-phonons. Microscopically this stems from the fact that LO-phonons couple to local charges through Coulomb interaction, that is physically the same quantity to which propagating electromagnetic waves couple. Only the particular choice of the Coulomb gauge makes them appear as distinct coupling mechanisms.

Polarons are also longitudinal excitations, being partially formed of LO-phonons, and as such their energies can be calculated with a simple dielectric function approach as the one sketched just above, if we take into account also the electronic component in the dielectric function. This approach is used, e.g., in Ref. [41]and it indeed gives the right results, also allowing to calculate all the optical observables of the system directly from the dielectric function.

Still physically such approach may appear rather unsatisfactory because, while allowing to calculate a number of physical observables, it completely neglects the microscopic nature of the coupling that creates the polarons. The polarons are due to the coupling of LO-phonons and electrons (Fröhlich interaction) and in the dielectric function approach, neither the LO-phonons, nor the Fröhlich interaction, are taken explicitly into account.

Apart from this rather formal considerations, missing a microscopic approach makes it difficult, or altogether impossible, to study what happens in more complex situations, as for example in inhomogeneous samples or when, due to the strength of the coupling, it could become possible to observe exotic phenomena as quantum vacuum effects or quantum phase transitions.

In the following sections we will develop a detailed microscopic theory for the intersubband transitions coupled to LO-phonons, in the Appendix we will compare the developed theory with the results of the standard dielectric function approach.

III. SUPERRADIANT EXCITATIONS

In 1954 Dicke[15] noticed that a set of coherently excited identical dipoles relaxes radiatively much faster than a single, isolated dipole. This is due to the phenomenon of superradiance: N identical dipoles behave as a single collective dipole $\sqrt{N}$ times bigger.

The reason of such collective enhancement can be understood considering that, being all the dipoles identical, all the transitions are degenerate and a simple basis change allows us to describe the system of N dipoles as a single superdipole coupled to the electromagnetic field and $N-1$ other modes that are not coupled to the field. The particular superposition that couples to the field (usually called *bright* mode) thus concentrates all the oscillator strength and has a dipole $\sqrt{N}$ times bigger.

The concept of superradiance has been thoroughly applied to the study of intersubband polaritons[18,42–44] in microcavity embedded doped quantum wells. In quantum wells the confinement of electrons along the growth direction splits the electron bands, giving rise to multiple parallel subbands. Being the subbands parallel, and being the electromagnetically induced transitions between them almost vertical (the wavevectors of the photons are negligible compared to the ones of the electrons), the situation is very similar to the one considered initially by Dicke. The N electrons that populate the lower conduction subband can jump vertically in the excited one and indeed can be considered as N independent dipoles. As expected[16,17], in these systems the strength of the coupling between light and matter is proportional to the square root of the number of electrons in the quantum well.

In this paper we will not consider the coupling of intersubband transitions with light, but we will study instead their coupling with longitudinal optical phonons, considering also the role of Coulomb electron-electron interaction. Such couplings are extremely rich and, in order to limit the complexity of our investigation, we will need to determine which scattering channels are dominant and which are negligible. Given that, in general, if N electrons undergo a certain transition in a coherent way the strength of the coupling is enhanced by a factor $\sqrt{N}$, transitions involving a macroscopic number of electrons will be treated exactly, while the others (involving only few electrons) will be treated perturbatively (or ignored altogether).

The degree of collective enhancement of a scattering process will be evaluated looking at the number of electrons that can participate to the process given fixed
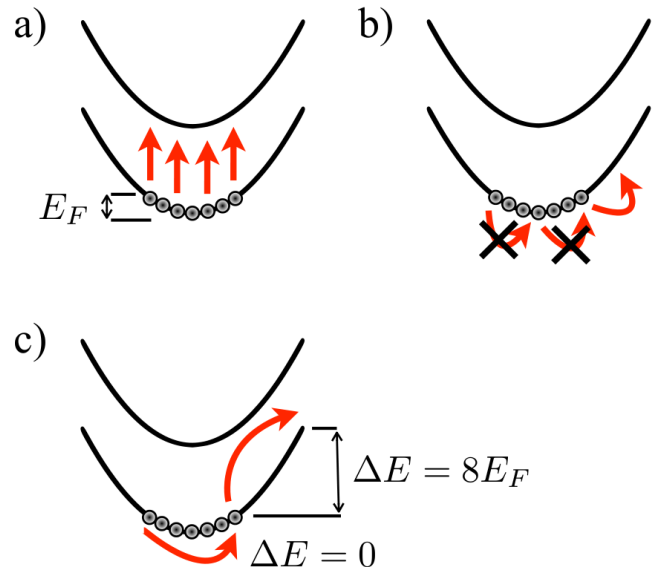

FIG. 1: a) An example of collective transition: an intersubband transition with small transferred momentum. b) An example of non-collective transition: an intrasubband transition with small transferred momentum in which most of the single particle transitions are Pauli blocked. c) An example of non-collective transition: an intrasubband transition with large transferred momentum. The extrema of the energy spread of single particle transitions are shown explicitly.

amounts of transferred impulsion and energy. In Fig. 1 we show a few illustrative examples. Panel (a) represents a transition from the first to the second subband, with a negligible amount of transferred momentum. All electrons can undergo this transition approximately at the same energy. This process will thus benefit from a large superradiant enhancement factor, proportional to the square root of the total number of the electrons in the gas. Panel (b) and (c) represent two possible transitions within the first subband. In panel (b) the transferred momentum is much smaller than the Fermi momentum $\hbar k_F$ and the majority of electrons, being Pauli blocked, do not participate to the process. In panel (c) the transferred momentum is of the order of $2\hbar k_F$, the minimum to allow all the electrons to undergo a transition avoiding Pauli blocking. Anyway there is a large energy spread between the different single electron transitions. Electrons on the two opposite borders of the Fermi sea, with initial momenta $\pm\hbar k_F$ parallel to the transferred momentum, have initially the same energy $\frac{\hbar^2 k_F^2}{2m^*} = E_F$, where m^* is the electron effective mass and E_F the Fermi energy. After the transition they will end up with final momenta of $\hbar k_F$ and $3\hbar k_F$, corresponding to final energies $\frac{\hbar^2 k_F^2}{2m^*} = E_F$ and $\frac{9\hbar^2 k_F^2}{2m^*} = 9E_F$ respectively. This implies that, even if the transition is not blocked, only a small fraction of the single electron transitions can be resonant at the same time. In both cases, given that only few electrons can participate to the collective transitions, the superradiant

enhancement factor will be small.

IV. THEORETICAL FRAMEWORK

A. Free fields

We will consider a symmetric quantum well of length L_{QW} in a bulk of height L_{BK}, S will be the surface of the sample. For the moment, we will limit ourselves to the case of a single quantum well, the general case of multiple quantum wells will be addressed later in this Section.

The quantum well is supposed to be doped in such a way that its Fermi level is between the first and the second conduction subbands, separated between them by the intersubband gap energy $\hbar\omega_{12}$.

We will develop our theory using a zero temperature formalism ($T = 0$), anyway our results will remain quantitatively accurate while the thermal population of the second subband remains negligeable. Depending on material parameters and doping level, this could imply the necessity to perform experiments in different kinds of cryogenic environments.

Electron states will be indexed by the subband index j and by the value of the in-plane wavevector $\mathbf{k}$. Their wavefunctions will be given by

$$\psi_{j,\mathbf{k}}(\rho, z) = \chi_j(z)\frac{e^{i\mathbf{k}\rho}}{\sqrt{S}}, \quad j = 1, 2, \tag{4}$$

where, for simplicity, we will choose $\chi_j(z)$ to be real and, due to the symmetry of the quantum well, the $\chi_j(z)$ have well defined and opposite symmetry. Wavefunctions in Eq. (4) are chosen as basis for second quantization, the creation operator for an electron in the state described by Eq. (4) will be denoted as $c_{j,\mathbf{k}}^\dagger$. The free Hamiltonian of electron gas in the two considered subbands thus reads

$$H_{el} = \sum_{j=\{1,2\},\mathbf{k}} \hbar\omega_j(\mathbf{k})c_{j,\mathbf{k}}^\dagger c_{j,\mathbf{k}}, \tag{5}$$

where $\omega_1(\mathbf{k}) = \frac{\hbar^2 k^2}{2m^*}$ and $\omega_2(\mathbf{k}) = \omega_1(\mathbf{k}) + \omega_{12}$. In Eq. (5), as well as in the rest of this paper, we will omit the electron spin index. This is justified by the fact that all interactions we consider are spin conserving. Given that we will consider only in-plane wavevector exchanges $\mathbf{q}$ much smaller than the typical electron wavevector $\mathbf{k}$, we can make the approximation $\omega_j(\mathbf{k}+\mathbf{q}) \simeq \omega_j(\mathbf{k})$, and introduce the operators describing intersubband transitions with a well defined and dispersionless energy $\hbar\omega_{12}$[16,17]

$$b_{\mathbf{q}}^\dagger = \frac{1}{\sqrt{N}}\sum_{\mathbf{k}} c_{2,\mathbf{k}+\mathbf{q}}^\dagger c_{1,\mathbf{k}}, \tag{6}$$

$$b_{\mathbf{q}} = \frac{1}{\sqrt{N}}\sum_{\mathbf{k}} c_{1,\mathbf{k}}^\dagger c_{2,\mathbf{k}+\mathbf{q}},$$

where N is the number of electrons in the quantum well. The $b_{\mathbf{q}}^\dagger$ operators are bosonic in the dilute regime[45], that

is, if there are n of such excitations in the system

$$[b_{\mathbf{q}}, b_{\mathbf{q}'}^\dagger] = \delta_{\mathbf{q},\mathbf{q}'} + O(\frac{n}{N}) \simeq \delta_{\mathbf{q},\mathbf{q}'}. \tag{7}$$

Using Eq. (6) we can rewrite the Hamiltonian of the free electron gas in Eq. (5) in terms of bosonic intersubband excitations

$$H_{el} = \sum_{\mathbf{q}} \hbar\omega_{12}b_{\mathbf{q}}^\dagger b_{\mathbf{q}}. \tag{8}$$

In this work we are interested in the resonant case in which ω_{12} is equal, or close, to the LO-phonon frequency ω_{LO}. We can thus neglect confinement effects on the phonons and consider bulk values for their frequencies[46,47]. We will thus describe LO-phonons by means of the three dimensional boson operators $d_{\mathbf{q},q_z}$

$$[d_{\mathbf{q},q_z}, d_{\mathbf{q}',q_z'}^\dagger] = \delta_{\mathbf{q},\mathbf{q}'}\delta_{q_z,q_z'}, \tag{9}$$

indexed by their in-plane and out-of-plane wavevectors. While we know that LO-phonon modes are confined inside the quantum well, we do not need to impose this constraint in the mode definition because, as we will see, intersubband transitions end up coupling with linear superpositions of phonon modes that are anyway confined inside the quantum well. We will consider only the case of one single longitudinal optical branch, the expansion to the case of multiple branches not presenting any fundamental difficulty.

Moreover, we are interested only in phonons with small in-plane wavevectors (in order to couple with coherent intersubband excitations), we can thus ignore phonon dispersion and write the free phonon Hamiltonian as

$$H_{ph} = \sum_{\mathbf{q},q_z} \hbar\omega_{LO}d_{\mathbf{q},q_z}^\dagger d_{\mathbf{q},q_z}. \tag{10}$$

B. Electron phonon interaction

Interaction between electrons and LO-phonons can be described using the Fröhlich Hamiltonian[3]

$$H_{Fr} = \sqrt{\frac{\hbar\omega_{LO}e^2}{2\epsilon_0\epsilon_\rho SL_{BK}}}\sum_{\mathbf{q},q_z}\frac{e^{-i(\mathbf{q}\rho+q_z z)}}{\sqrt{q^2+q_z^2}}d_{\mathbf{q},q_z}^\dagger + h.c., \tag{11}$$

where

$$\frac{1}{\epsilon_\rho} = \frac{1}{\epsilon_\infty} - \frac{1}{\epsilon_s}, \tag{12}$$

and ϵ_s and ϵ_∞ are respectively the static and high frequency dielectric constants[47].

The Hamiltonian in Eq. (11) can be written in second quantization (neglecting incoherent intrasubband scattering[34]) as

$$\begin{aligned} H_{Fr} = &\sqrt{\frac{\hbar\omega_{LO}e^2}{2\epsilon_0\epsilon_\rho SL_{BK}}}\sum_{\mathbf{q},q_z}\frac{F(q_z)}{\sqrt{q^2+q_z^2}} \\ &(d_{\mathbf{q},q_z}^\dagger + d_{-\mathbf{q},-q_z})(c_{1,\mathbf{k}}^\dagger c_{2,\mathbf{k}+\mathbf{q}} + c_{2,\mathbf{k}-\mathbf{q}}^\dagger c_{1,\mathbf{k}}), \end{aligned} \tag{13}$$

where we have defined

$$F(q) = \int dz \chi_1(z)\chi_2(z)e^{-iqz}. \quad (14)$$

From Eq. (13) we see that, due to the three dimensional character of the LO-phonons[47], each electronic transition couples to multiple phonon modes, indexed by different values of the wavevector along the growth direction. It is thus convenient to introduce second quantized operators corresponding to the particular linear superposition of phonon modes that are coupled to electronic transitions

$$r_{\mathbf{q}}^\dagger = \frac{1}{\sqrt{A}} \sum_{q_z} \frac{F(q_z)d_{\mathbf{q},q_z}^\dagger}{\sqrt{q^2+q_z^2}},$$

$$r_{\mathbf{q}} = \frac{1}{\sqrt{A}} \sum_{q_z} \frac{\bar{F}(q_z)d_{\mathbf{q},q_z}}{\sqrt{q^2+q_z^2}}, \quad (15)$$

whose spatial wavefunctions along the z axis is

$$\varphi_q(z) = \frac{1}{\sqrt{AL_{BK}}} \sum_{q_z} \frac{F(q_z)e^{iq_z z}}{\sqrt{q^2+q_z^2}}. \quad (16)$$

From Eqs. (16) and (14) we see that the intersubband transitions naturally couple to phonon modes localized inside the quantum well (it is easy to verify that $\varphi_q(z)$ vanishes to the first order in q if z is outside the common support of χ_1 and χ_2).

The normalization factor A can be fixed imposing bosonic commutation relations to the $r_{\mathbf{q}}^\dagger$ operators

$$[r_{\mathbf{q}}, r_{\mathbf{q}'}^\dagger] = \frac{1}{A} \sum_{q_z,q_z'} \frac{F(q_z)F(-q_z')}{\sqrt{(q^2+q_z^2)(q'^2+q_z'^2)}}[d_{\mathbf{q},q_z}, d_{\mathbf{q}',q_z'}^\dagger]$$

$$= \frac{\delta_{\mathbf{q},\mathbf{q}'}L_{BK}I(q)}{2Aq}, \quad (17)$$

and thus

$$A = \frac{L_{BK}}{2}\frac{I(q)}{q}, \quad (18)$$

where we have defined

$$I(q) = \int dz dz' \chi_1(z)\chi_2(z)\chi_2(z')\chi_1(z')e^{-q|z-z'|}. \quad (19)$$

We can thus write Hamiltonians in Eq. (10) and Eq. (13) in term of coherent $r_{\mathbf{q}}^\dagger$ and $b_{\mathbf{q}}^\dagger$ operators as

$$H_{ph} = \sum_{\mathbf{q}} \hbar\omega_{LO}r_{\mathbf{q}}^\dagger r_{\mathbf{q}}, \quad (20)$$

and

$$H_{Fr} = \sum_{\mathbf{q}} \sqrt{N_{2DEG}\hbar\omega_{LO}\frac{e^2}{4\epsilon_0\epsilon_\rho}\frac{I(q)}{q}}(b_{\mathbf{q}}^\dagger + b_{-\mathbf{q}})(r_{\mathbf{q}} + r_{-\mathbf{q}}^\dagger),$$
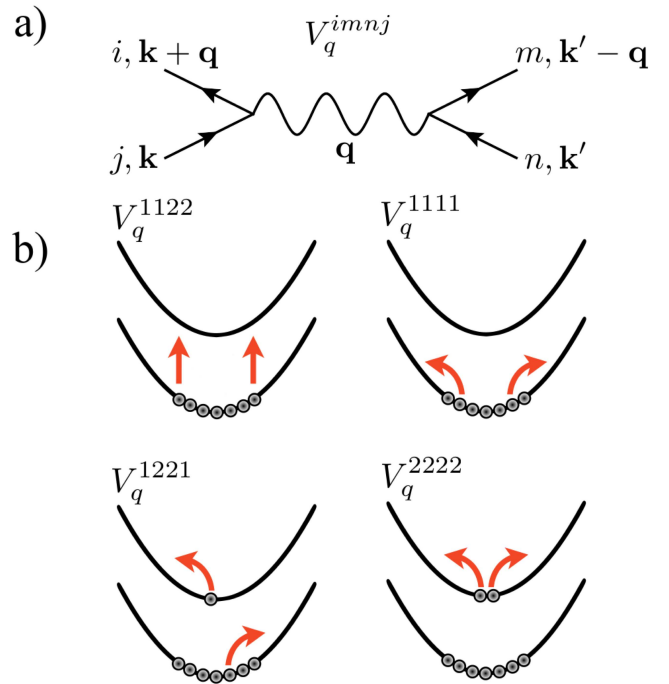

FIG. 2: a) Graphical representation of the scattering channel V_q^{imnj}. Two electrons in subbands j and n, with momenta $\mathbf{k}$ and $\mathbf{k}'$ are scattered into subbands i and m, with momenta $\mathbf{k}+\mathbf{q}$ and $\mathbf{k}'-\mathbf{q}$ respectively.

where

$$N_{2DEG} = \frac{N}{S}, \quad (21)$$

is the density of the two dimensional electron gas inside the quantum well. In order to pass from Eq. (10) to Eq. (20), we are neglecting higher order phonon modes confined inside the quantum well. This is justified by the fact that we limit ourselves to long-wavelength modes.

C. Resonant Electron-Electron interaction

In order to treat the Coulomb electron-electron interaction we start by the second quantized form of the Hamiltonian describing the Coulomb interaction[48] (see Fig. 2 (a) for a graphical representation of the interaction coefficients)

$$H_c = \frac{1}{2} \sum_{i,j,m,n=1,2} \sum_{\mathbf{q},\mathbf{k},\mathbf{k}'} V_q^{imnj}c_{i,\mathbf{k}+\mathbf{q}}^\dagger c_{m,\mathbf{k}'-\mathbf{q}}^\dagger c_{n,\mathbf{k}'}c_{j,\mathbf{k}}, \quad (22)$$

where

$$V_q^{imnj} = \frac{e^2}{2\epsilon_0\epsilon_\infty q} \int dz dz' \chi_i(z)\chi_j(z)\chi_m(z')\chi_n(z')e^{-q|z-z'|},$$
$$(23)$$

is the two dimensional Coulomb matrix element. It is important to notice that in Eq. (23) we used the high

frequency dielectric constant ϵ_∞ instead of the static one. This is due to the fact that ϵ_s includes the effect of the coupling to LO-phonons, that is already treated exactly in the Hamiltonian.

Due to the symmetry of the wavefunctions, a certain number of matrix elements in Eq. (23) can be seen to be zero, in particular all the matrix elements with an odd number of 1 and 2 indices

$$V_q^{1112} = V_q^{1121} = V_q^{1211} = V_q^{2111} = 0, \qquad (24)$$
$$V_q^{2111} = V_q^{2212} = V_q^{2122} = V_q^{1222} = 0.$$

The other elements can be evaluated as

$$V_q^{1122} = V_q^{1212} = V_q^{2121} = V_q^{2211} = \frac{e^2 I(q)}{2\epsilon_0 \epsilon_\infty q}, \qquad (25)$$

$$V_q^{1221} = V_q^{2112} = \frac{e^2}{2\epsilon_0 \epsilon_\infty q} \int dz dz' \chi_1^2(z) \chi_2^2(z') e^{-q|z-z'|},$$

$$V_q^{1111} = \frac{e^2}{2\epsilon_0 \epsilon_\infty q} \int dz dz' \chi_1^2(z) \chi_1^2(z') e^{-q|z-z'|},$$

$$V_q^{2222} = \frac{e^2}{2\epsilon_0 \epsilon_\infty q} \int dz dz' \chi_2^2(z) \chi_2^2(z') e^{-q|z-z'|},$$

where $I(q)$, defined in Eq. (19), is same integral we encountered studying the electron-phonon Fröhlich interaction.

The four distinct nonzero possible values of the matrix elements correspond to different kinds of scattering processes. In Fig. 2 (b) a graphical representation for each of these processes is shown.

It is important at this point to notice a major difference between the elements in the first line of Eq. (25) and the others. The elements in the first line (upper left subpanel in Fig. 2 (b)) represent intersubband excitations: each electron is scattered from one subband to the other. Such processes, responsible for the depolarization shift[48], describe a superradiant process in the sense defined in Sec. III, that is, at least for small values of $\mathbf{q}$, a great number of electrons can coherently undergo the same transition, approximately at the same energy. This is not the case for the interactions described in the other lines of Eq. (25), that instead describe intrasubband excitations that, either due to Pauli blocking or to the non-flat energy dispersion, involve only few electrons (see Fig. 1).

The discussion in Sec. III thus implies that the strength of the terms in the first line of Eq. (25) strongly dominates over the others due to the superradiant enhancement. For this reason we have to treat them exactly in an Hamiltonian formalism, while we can limit ourselves to treat the others within a perturbative approach.

Here we will thus construct an exact, Hamiltonian approach, to treat the effect of the depolarization shift terms, neglecting the others. We will analyze later the effect of the intrasubband terms.

Le us start to rewrite the depolarization shift part of Eq. (22) in a more useful form

$$
\begin{aligned}
H_c &= \sum_{\mathbf{q},\mathbf{k},\mathbf{k}'} \frac{e^2 I(q)}{4\epsilon_0 \epsilon_\infty q} \left(c_{1,\mathbf{k}+\mathbf{q}}^\dagger c_{1,\mathbf{k}'-\mathbf{q}}^\dagger c_{2,\mathbf{k}'} c_{2,\mathbf{k}} + c_{1,\mathbf{k}+\mathbf{q}}^\dagger c_{2,\mathbf{k}'-\mathbf{q}}^\dagger c_{1,\mathbf{k}'} c_{2,\mathbf{k}} + c_{2,\mathbf{k}+\mathbf{q}}^\dagger c_{1,\mathbf{k}'-\mathbf{q}}^\dagger c_{2,\mathbf{k}'} c_{1,\mathbf{k}} + c_{2,\mathbf{k}+\mathbf{q}}^\dagger c_{2,\mathbf{k}'-\mathbf{q}}^\dagger c_{1,\mathbf{k}'} c_{1,\mathbf{k}} \right) \\
&= \sum_{\mathbf{q},\mathbf{k},\mathbf{k}'} \frac{e^2 I(q)}{4\epsilon_0 \epsilon_\infty q} \left(c_{1,\mathbf{k}+\mathbf{q}}^\dagger c_{2,\mathbf{k}} c_{1,\mathbf{k}'-\mathbf{q}}^\dagger c_{2,\mathbf{k}'} + c_{1,\mathbf{k}+\mathbf{q}}^\dagger c_{2,\mathbf{k}} c_{2,\mathbf{k}'-\mathbf{q}}^\dagger c_{1,\mathbf{k}'} + c_{2,\mathbf{k}+\mathbf{q}}^\dagger c_{1,\mathbf{k}} c_{1,\mathbf{k}'-\mathbf{q}}^\dagger c_{2,\mathbf{k}'} + c_{2,\mathbf{k}+\mathbf{q}}^\dagger c_{1,\mathbf{k}} c_{2,\mathbf{k}'-\mathbf{q}}^\dagger c_{1,\mathbf{k}'} \right) \\
&\quad + \sum_{\mathbf{q}} \frac{N e^2 I(q)}{4\epsilon_0 \epsilon_\infty q}.
\end{aligned}
\qquad (26)
$$

We see from Eq. (26) that, thanks to its collective, superradiant nature, the depolarization shift can be naturally written in terms of the bosonic intersubband excitations defined in Eq. (6) as

$$H_c = \sum_{\mathbf{q}} N_{2DEG} \frac{e^2}{4\epsilon_0 \epsilon_\infty} \frac{I(q)}{q} (b_{\mathbf{q}}^\dagger + b_{-\mathbf{q}})(b_{-\mathbf{q}}^\dagger + b_{\mathbf{q}}), \quad (27)$$

where we have neglected the last constant term, that simply shifts the ground state energy.

D. Residual Electron-Electron interaction

We showed how it is possible to treat exactly the depolarization shift effect in a bosonic excitation formalism. It remains to study the effect of the residual Coulomb contributions due to the intrasubband terms in the last three lines of Eq. (25) (schematized in the last three panels of Fig. 2 (b)).

An important result due to Lee and Galbraith[49,50], is that such intrasubband terms do not contribute to the screening of the intersubband ones at the level of the random phase approximation (RPA). This can be seen

writing the Dyson equation for the dynamically screened Coulomb potential[51] $\mathcal{V}_q(\omega)$

$$\mathcal{V}_q^{imnj}(\omega) = V_q^{imnj} + \sum_{rs} V_q^{irsj}\Pi_q^{sr}(\omega)\mathcal{V}_q^{smnr}(\omega), \quad (28)$$

where $\Pi_{sr}(q,\omega)$ is the RPA polarization function. In the case of an intersubband contribution (e.g. $\mathcal{V}_q^{1122}$), Eqs. (24) and (25) imply that

$$\begin{aligned}\mathcal{V}_q^{1122}(\omega) &= V_q^{1122} + \sum_{rs} V_q^{1rs2}\Pi_q^{sr}(\omega)\mathcal{V}_q^{s12r}(\omega) \quad (29)\\ &= V_q^{1122} + \sum_{r\neq s} V_q^{1rs2}\Pi_q^{sr}(\omega)\mathcal{V}_q^{s12r}(\omega)\\ &= V_q^{1122} + V_q^{1122}(\Pi_q^{12}(\omega) + \Pi_q^{21}(\omega))\mathcal{V}_q^{1122}(\omega).\end{aligned}$$

We have thus

$$\mathcal{V}_q^{1122}(\omega) = \frac{V_q^{1122}}{1 - V_q^{1122}(\Pi_q^{12}(\omega) + \Pi_q^{21}(\omega))}, \quad (30)$$

from which we see that the intrasubband Coulomb terms ($V_q^{1111}, V_q^{2222}, V_q^{1221}$ and V_q^{2112}) do not intervene in the renormalization of the intersubband terms.

An analogous reasoning can be done for the phonon-electron interaction. Calling M_{q,q_z} and $\mathcal{M}_{q,q_z}(\omega)$ the bare and screened version of the potential defined in Eq. (13), we have the Dyson equation

$$\begin{aligned}\mathcal{M}_{q,q_z}(\omega) &= M_{q,q_z} + \sum_{rs} V_q^{1mn2}\Pi_q^{sr}(\omega)\mathcal{M}_{q,q_z}(\omega) \quad (31)\\ &= M_{q,q_z} + V_q^{1122}(\Pi_q^{12}(\omega) + \Pi_q^{21}(\omega))\mathcal{M}_{q,q_z}(\omega),\end{aligned}$$

and we have thus the formula for the screened potential

$$\mathcal{M}_{q,q_z}(\omega) = \frac{M_{q,q_z}}{1 - V_q^{1122}(\Pi_q^{12}(\omega) + \Pi_q^{21}(\omega))}. \quad (32)$$

Being the RPA screening only due to terms that are exactly treated in the Hamiltonian, we can thus neglect the screening due to the two dimensional electron gas.

E. Hopfield-Bogoliubov Hamiltonian

Putting together Eqs. (8), (21) and (27) we arrive to the full Hamiltonian for the intersubband transitions-LO-phonons system

$$\begin{aligned}H = &\sum_{\mathbf{q}} \hbar\omega_{12} b_{\mathbf{q}}^{\dagger} b_{\mathbf{q}} + \hbar\omega_{LO} r_{\mathbf{q}}^{\dagger} r_{\mathbf{q}} \quad (33)\\ &+ \sqrt{N_{2DEG}\hbar\omega_{LO}\frac{e^2}{4\epsilon_0\epsilon_\rho}\frac{I(q)}{q}}(b_{\mathbf{q}}^{\dagger} + b_{-\mathbf{q}})(r_{-\mathbf{q}}^{\dagger} + r_{\mathbf{q}})\\ &+ N_{2DEG}\frac{e^2}{4\epsilon_0\epsilon_\infty}\frac{I(q)}{q}(b_{\mathbf{q}}^{\dagger} + b_{-\mathbf{q}})(b_{-\mathbf{q}}^{\dagger} + b_{\mathbf{q}}).\end{aligned}$$

The Hamiltonian in Eq. (33) can be rewritten in a more compact form by introducing the intersubband transitions-LO-phonons coupling constant Ω and the depolarization shift constant D

$$\begin{aligned}\Omega &= \sqrt{N_{2DEG}\omega_{LO}\frac{e^2}{4\epsilon_0\epsilon_\rho\hbar}\frac{I(q)}{q}}, \quad (34)\\ D &= N_{2DEG}\frac{e^2}{4\epsilon_0\epsilon_\infty}\frac{I(q)}{q},\end{aligned}$$

where we have dropped the dependences over the wavevector as we are interested in the long wavelength limit (from Eq. (19) we can verify that $\lim_{q\to 0}\frac{I(q)}{q}$ tends to a constant value).

Using Eq. (34), Eq. (33) can be written as

$$\begin{aligned}H = &\hbar\sum_{\mathbf{q}} \omega_{12} b_{\mathbf{q}}^{\dagger} b_{\mathbf{q}} + \omega_{LO} r_{\mathbf{q}}^{\dagger} r_{\mathbf{q}} + \Omega(b_{\mathbf{q}}^{\dagger} + b_{-\mathbf{q}})(r_{-\mathbf{q}}^{\dagger} + r_{\mathbf{q}})\\ &+ D(b_{\mathbf{q}}^{\dagger} + b_{-\mathbf{q}})(b_{-\mathbf{q}}^{\dagger} + b_{\mathbf{q}}), \quad (35)\end{aligned}$$

that can be cast in matrix form as

$$H = \frac{\hbar}{2}\sum_{\mathbf{q}} \hat{v}_{\mathbf{q}}^{\dagger}\, \eta\, \mathcal{M}_q\, \hat{v}_{\mathbf{q}}, \quad (36)$$

where the column vector of operators $\hat{v}_{\mathbf{q}}$ is defined as

$$\hat{v}_{\mathbf{q}} = [b_{\mathbf{q}}, r_{\mathbf{q}}, b_{-\mathbf{q}}^{\dagger}, r_{-\mathbf{q}}^{\dagger}]^T, \quad (37)$$

η is the diagonal metric

$$\eta = \mathrm{diag}[1, 1, -1, -1], \quad (38)$$

and the Hopfield-Bogoliubov[52] matrix $\mathcal{M}_q$ is defined as

$$\mathcal{M}_q = \begin{pmatrix} \omega_{12} + 2D & \Omega & 2D & \Omega \\ \Omega & \omega_{LO} & \Omega & 0 \\ -2D & -\Omega & -\omega_{12} - 2D & -\Omega \\ -\Omega & 0 & -\Omega & -\omega_{LO} \end{pmatrix}. \quad (39)$$

Diagonalizing the matrix in Eq. (39) will yield the frequencies of the normal modes of the system $\omega_{\pm}$, that are usually called polarons[32,33]. In our case we will name them more properly intersubband polarons, because the electronic part of the mixed excitation is given by an intersubband transition.

It is interesting to notice that, from Eq. (34), we can write the Coulomb coefficient D as

$$D = \frac{\Omega^2}{\omega_{LO}}\frac{\epsilon_\rho}{\epsilon_\infty} \geq \frac{\Omega^2}{\omega_{LO}}. \quad (40)$$

As it has recently been shown in Ref. [53], Eq. (40) implies that it is impossible to observe a Dicke phase transition in the system we are considering, regardless of the strength of the coupling.

F. Multiple Quantum Wells

Until now we considered the case of a single quantum well. This choice has been motivated by the fact that,

as we will show, the presence of multiple quantum wells does not modify our results.

Given that we are considering rather large quantum wells (in order for the transition to be resonant with the LO-phonon mode), the optical phonon spectrum is not modified[47] and the optical phonon modes we consider are confined in each quantum well.

This is a rather important difference between the intersubband polaron case we consider in this paper and the physics of intersubband polaritons. For intersubband polaritons, the electromagnetic mode coupled to the intersubband transitions extends over all the quantum wells in the structure. It thus couples to all the electrons, regardless of the quantum well they are in. This means that the only meaningful parameter for intersubband polaritons is the total density of electrons, and the light-matter coupling thus scales as $\sqrt{n_{QW} N_{2DEG}}$, where n_{QW} is the number of quantum wells inside the microcavity.

In the present case instead, being the phonon modes confined inside each quantum well, electrons in different quantum wells are completely decoupled. This can also be inferred from the coupling integral in Eq. (23). This integral does vanish, at least in the long wavelength limit (first order in q), if the wavefunctions for the two integration variables z and z' do not have a common support, i.e., if the two interacting electrons are in different quantum wells.

This means that, contrary to the intersubband polariton case, the intersubband polaron interaction scales only as $\sqrt{N_{2DEG}}$ and growing multiple quantum wells in the same sample will not increase the coupling.

V. RESULTS

In order to obtain some numerical predictions from Hamiltonian in Eq. (35), we need to fix a few parameters concerning the material and the quantum well.

For sake of simplicity we will consider the quantum well to be correctly approximated by a rectangular, infinite potential well of length L_{QW}. We thus have

$$\hbar\omega_{12} = \frac{3\hbar^2\pi^2}{2m^* L_{QW}^2},\qquad(41)$$

and the electronic and phononic modes profiles are given by

$$\chi_1(z) = \sqrt{\frac{2}{L_{QW}}}\sin(\frac{\pi z}{L_{QW}}),\qquad(42)$$

$$\chi_2(z) = \sqrt{\frac{2}{L_{QW}}}\sin(\frac{2\pi z}{L_{QW}}),$$

$$\varphi_0(z) = \sqrt{\frac{16}{5L_{QW}}}\sin^3(\frac{\pi z}{L_{QW}}),$$

$$(43)$$

inside the quantum well and zero outside. As explained in Sec. IV, we see here explicitly that the intersubband transitions couple to a linear superposition of phonon modes that is localized inside the quantum well (the cubic sinus in the third line of Eq. (42) comes from the integral of the two first two, as can be verified performing the integral in Eq. (16)).

Inserting Eq. (42) into Eq. (19) and performing the integral we have

$$\lim_{q\to 0} I(q) \to \frac{10}{9\pi^2} q L_{QW}.\qquad(44)$$

In Fig. 3 we plot the normalized coupling $\frac{\Omega}{\omega_{LO}}$ as a function of the two dimensional electron gas, for a GaAs quantum well. In the inset of Fig. 3 we instead present a comparison of the values of $\frac{\Omega}{\omega_{LO}}$, at room temperature, for different semiconductors of the III-V and II-VI groups[54], as a function of the respective LO-phonon energies, for a reference doping $N_{2DEG} = 10^{12}\text{cm}^{-2}$.

In Fig. 4 there is a plot of the intersubband polaron frequencies $\omega_\pm$ as a function of the intersubband frequency ω_{12}, in GaAs, for $N_{2DEG} = 10^{12}\text{cm}^{-2}$. Notice that, due to the effect of Coulomb interaction, the resonant anticrossing is not at $\omega_{12} = \omega_{LO}$ but at a lower frequency. In the inset of the same figure we plot the same quantity as a function of the electron density. The quantum well length L_{QW} has been chosen in this case to have the two uncoupled modes at resonance ($\omega_{12} = \omega_{LO}$, that is $L_{QW} \simeq 23$nm).

It is clear from the figure that intersubband polarons are not only strongly coupled, having coupling constants much larger than their linewidth (usual linewidths being not bigger than a few meV), but they are indeed in the ultrastrong coupling regime, with values of the renormalized coupling $\frac{\Omega}{\omega_{LO}}$ comparable or larger than the best ones reported in the literature[21]. For physically realizable levels of doping, coupling values of a few tenths of the bare frequency of the excitation ω_{LO} are predicted in GaAs, and it seems that values much larger can be obtained using more polar materials. The reason of such large coupling can be found in the superradiant nature of intersubband excitations and in the natural confinement of the phonons inside the quantum well, that gives an extremely small mode volume, when compared with what can be obtained with photonic microcavities.

The consequences of our results can be multiple, both for fundamental and applied research. On the fundamental side, intersubband polarons could become a new laboratory to test quantum vacuum physics, typical of the ultrastrong coupling regime[28]. On the applied side our theory can be naturally exploited in the study of quantum cascade lasers working in or near the Restrahlen band. It can, for example, help explaining the anticrossing observed in Ref. 36, near the LO-phonon frequency. Moreover the capability to strongly modify the LO-phonon spectrum could have an impact on the performances of optoelectronic devices, as the electron-LO-phonon scattering rate determines the lifetime of carriers in excited
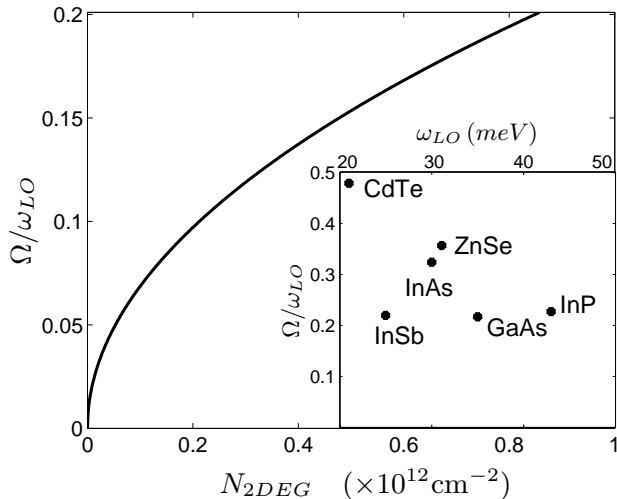
FIG. 3: Normalized coupling $\frac{\Omega}{\omega_{LO}}$ in GaAs as a function of the doping density N_{2DEG}. Inset: the same quantity as a function of the LO-phonon frequency ω_{LO} for different materials, for $N_{2DEG} = 10^{12} \text{cm}^{-2}$.
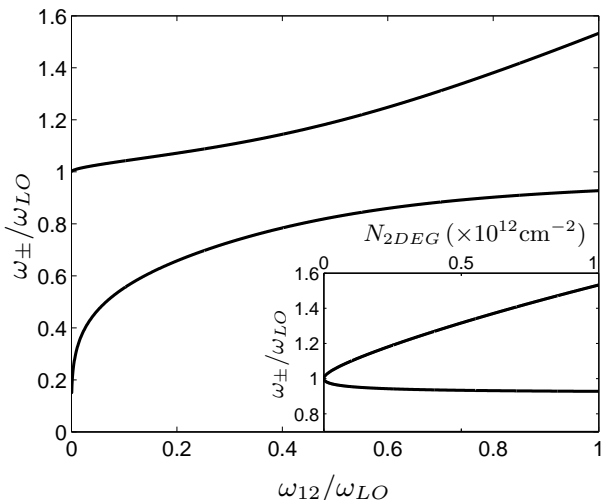

FIG. 4: Intersubband polaron frequencies $\omega_\pm$ as a function of the intersubband frequency ω_{12} for GaAs. Inset: the same quantity as a function of the doping for $\omega_{12} = \omega_{LO}$.

subbands[34].

VI. CONCLUSIONS

In this paper we have developed a microscopic theory of intersubband polarons, mixed excitations resulting from the coupling between intersubband transitions in doped quantum wells and LO-phonons. We took into account the electron-electron Coulomb interaction and we were able to treat exactly the resulting depolarization

shift. We proved that intersubband polarons can be in the ultrastrong coupling regime, reaching extremely high values of the coupling constant. We critically discussed the relevance of our result both for fundamental and applied research.

VII. ACKNOWLEDGMENTS

Appendix: Comparison with dielectric function theory

As explained in Sec. II, the dispersion of intersubband polarons can be calculated by solving Eq. (3) for the dielectric function of the coupled quantum well-lattice system. In order to test our theory we will compare this approach, following what done in Ref. [41], with the microscopic one we developed in this manuscript.

The total dielectric function of the system is given by[21,41]

$$\epsilon(\omega) = \epsilon_\infty \frac{\omega^2 - \omega_{LO}^2}{\omega^2 - \omega_{TO}^2 + i\omega 0^+} - \epsilon_\infty \frac{\omega_P^2}{\omega^2 - \omega_{12}^2 + i\omega 0^+}, \tag{45}$$

where

$$\omega_P^2 = \frac{2\omega_{12}d_{12}^2 N_{2DEG}}{\hbar\epsilon_0\epsilon_\infty L_{QW}}, \tag{46}$$

is the plasma frequency of the two dimensional electron gas and d_{12} is the intersubband dipole

$$d_{12} = e \int dz \chi_1(z) z \chi_2(z). \tag{47}$$

The equation

$$\Re[\epsilon(\omega)] = 0, \tag{48}$$

thus reads

$$\omega^4 - \omega^2(\omega_{LO}^2 + \omega_{12}^2 + \omega_P^2) + \omega_{LO}^2\omega_{12}^2 + \omega_{TO}^2\omega_P^2 = 0. \tag{49}$$

Note that Eq. (45) refers to the dipolar function along the z direction. In order to recover the same result from our microscopic approach, we will thus have to consider only $\mathbf{q} = 0$ phonons. Moreover, the use of a simple dielectric function theory, requires to have an homogeneous medium. This is equivalent to consider only the mode with $q_z \to 0$, that is, from Eqs. (14) and (47)

$$\frac{F(q_z)}{\sqrt{q^2 + q_z^2}} \to -i\frac{d_{12}}{e}. \tag{50}$$

Following exactly the same procedure done in Sec. IV, but with the $F(q)$ defined in Eq. (50) and considering only the $q_z \to 0$ mode, we get

$$\Omega = \sqrt{\frac{N_{2DEG}\omega_{LO}d_{12}^2}{2\epsilon_0\epsilon_\rho L_{QW}\hbar}}, \qquad (51)$$

and thus, from Eq. (40)

$$D = \frac{N_{2DEG}d_{12}^2}{2\epsilon_0\epsilon_\infty L_{QW}\hbar}. \qquad (52)$$

In order to obtain the polaronic eigenfrequencies we have to diagonalize the matrix in Eq. (39) using the coupling coefficients for the homogeneous limit defined in Eqs. (51) and (52). We thus obtain the secular equation

$$\omega^4 - \omega^2(\omega_{LO}^2 + \omega_{12}^2 + 4D\omega_{12}) \qquad (53)$$
$$+\omega_{LO}^2\omega_{12}^2 + 4D\omega_{12}\omega_{LO}^2 - 4\Omega^2\omega_{12}\omega_{LO} = 0,$$

that, using Eqs. (52) and (46) can be put into the form

$$\omega^4 - \omega^2(\omega_{LO}^2 + \omega_{12}^2 + \omega_P^2) + \omega_{LO}^2\omega_{12}^2 + \omega_P^2\omega_{LO}^2\frac{\epsilon_\infty}{\epsilon_s} = 0. \qquad (54)$$

Equating the coefficients of Eqs. (49) and (54), we obtain

$$\omega_{TO}^2 = \omega_{LO}^2\frac{\epsilon_\infty}{\epsilon_s}, \qquad (55)$$

that is the well known Lyddane-Sachs-Teller relation[47]. We have thus proved that the homogeneous version of our theory gives the same results as the homogeneous dielectric function approach.

It is anyway important to notice that the homogeneous limit in not exact, as a quantum well is, by definition, non-homogeneous. Ignoring the higher q_z modes leads to underestimate the intersubband dipole of a factor roughly equal to $\sqrt{2}$.

[1] L. D. Landau, Phys. Z. Sovjet **3**, 664 (1933).
[2] J. T. Devreese, Encyclopedia of Applied Physics **14**, 383 (1996).
[3] H. Fröhlich, Adv. Phys. **3**, 325 (1954).
[4] X. G. Wu, F. M. Peeters and J. T. Devreese, Phys. Rev. B **34**, 2621 (1986).
[5] F. M. Peeters and J. T. Devreese, Phys. Rev. B *36*, 4442 (1987).
[6] R. P. Feynman, Phys. Rev. **97**, 660 (1955).
[7] S. J. Miyake, J. Phys. Soc. Japan **38**,181 (1975).
[8] G. D. Mahan, *Many Particle Physics*, Springer (2000).
[9] B. B.Varga, Phys. Rev. **D7**, A1896 (1965).
[10] K. S. Singwi and M. P. Tosi, Phys. Rev. **147**, 658 (1966).
[11] A. Mooradian and A. L. McWhorter, Phys. Rev. Lett. **19**, 849 (1967).
[12] C. G. Olson and D. W. Lynch, Phys. Rev. **177**, 1231 (1968).
[13] S. Haroche and J.-M. Raimond, *Exploring the Quantum: Atoms, Cavities, and Photons*, Oxford University Press (2006).
[14] M. Devoret, S. Girvin, R. Schoelkopf, Ann. Phys. (Leipzig) **16**, 767 (2007).
[15] R. H. Dicke, Phys. Rev. **93**, 99 (1954).
[16] C. Ciuti, G. Bastard and I. Carusotto, Phys. Rev. B **72**, 115303 (2005).
[17] C. Ciuti and I. Carusotto, Phys. Rev. A **74**, 033811 (2006).
[18] D. Dini, R. Kohler, A. Tredicucci, G. Biasiol and L. Sorba, Phys. Rev. Lett. **90**, 116401 (2003).
[19] G. Günter, A. A. Anappara, J. Hees, A. Sell, G. Biasiol, L. Sorba, S. De Liberato, C. Ciuti, A. Tredicucci, A. Leitenstorfer and R. Huber, Nature (London) **458**, 178 (2009).
[20] A. A. Anappara, S. De Liberato, A. Tredicucci, C. Ciuti, G. Biasiol, L. Sorba and F. Beltram, Phys. Rev. B **79**, 201303 (2009).
[21] Y. Todorov, A. M. Andrews, R. Colombelli, S. De Liberato, C. Ciuti, P. Klang, G. Strasser and C. Sirtori, Phys. Rev. Lett. **105**, 196402 (2010).
[22] J. Bourassa, J. M. Gambetta, A. A. Abdumalikov, Jr., O. Astafiev, Y. Nakamura and A. Blais, Phys. Rev. A **80**, 032109 (2009).
[23] T. Niemczyk, F. Deppe, H. Huebl, E. P. Menzel, F. Hocke, M. J. Schwarz, J. J. Garcia-Ripoll, D. Zueco, T. Hümmer, E. Solano, A. Marx and R. Gross, Nat. Phys. **6**, 772 (2010).
[24] T. Schwartz, J. A. Hutchison, C. Genet and T. W. Ebbesen, Phys. Rev. Lett. **106**, 196405 (2011).
[25] D. Hagenmüller, S. De Liberato and C. Ciuti, Phys. Rev. B **81**, 235303 (2010).
[26] G. Scalari, C. Maissen, D. Turcinková, D. Hagenmüller, S. De Liberato, C. Ciuti, D. Schuh, C. Reichl, W. Wegscheider, M. Beck and J. Faist, arXiv:1111.2486.
[27] M. Kardar and R. Golestanian, Rev. Mod. Phys. **71**, 1233 (1999).
[28] S. De Liberato, C. Ciuti and I. Carusotto, Phys. Rev. Lett. **98**, 103602 (2007).
[29] S. De Liberato, D. Gerace, I. Carusotto and C. Ciuti, Phys. Rev. A **80**, 053810 (2009).
[30] C. Emary and T. Brandes, Phys. Rev. Lett. **90**, 044101 (2003).
[31] N. Lambert, C. Emary and T. Brandes, Phys. Rev. Lett. **92**, 073602 (2004).
[32] O. Verzelen, R. Ferreira and G. Bastard, Phys. Rev. Lett. **88**, 146803 (2002).
[33] S. Hameau, Y. Guldner, O. Verzelen, R. Ferreira, G. Bastard, J. Zeman, A. Lemaître and J. M. Gérard, Phys. Rev. Lett. **83**, 4152 (1999).
[34] R. Ferreira and G. Bastard, Phys. Rev. B **40**, 1074 (1989).
[35] J. Faist, F. Capasso, D. L. Sivco, C. Sirtori, A. L. Hutchinson and A. Y. Cho, Science **264**, 5158 (1994).
[36] F. Castellano, A. Bismuto, M. I. Amanti, R. Terazzi, M. Beck, S. Blaser, A. Bächle and J. Faist, J. App. Phys. **109**, 102407 (2011).
[37] R. Colombelli, F. Capasso, C. Gmachl, A. L. Hutchinson, D. L. Sivco, A. Tredicucci, M. C. Wanke, A. M. Sergent and A. Y. Cho, Appl. Phys. Lett., **78**, 2620 (2001).
[38] S. Butscher, J. Forstner, I. Waldmuller and A. Knorr, Phys. Stat. Sol. B **241**, 11 (2004).

[39] S. Butscher and A. Knorr, Phys. Rev. Lett. **97**, 197401 (2006).

[40] J. C. Cao, Y. L. Chen and H. C. Liu, Superlattices and Microstructures **40**, 119 (2006).

[41] H. C. Liu, C. Y. Song, Z. R.Wasilewski, A. J. SpringThorpe, J. C. Cao, C. Dharma-wardana, G. C. Aers, J. Lockwood and J. A. Gupta, Phys. Rev. Lett. **90**, 077402 (2003).

[42] A. Anappara, A. Tredicucci, F. Beltram, G. Biasiol, L. Sorba, S. De Liberato and C. Ciuti, App. Phys. Lett. **91**, 231118 (2007).

[43] L. Sapienza, A. Vasanelli, C. Ciuti, C. Manquest, C. Sirtori, R. Colombelli and U. Gennser, App. Phys. Lett. **90**, 201101 (2007).

[44] L. Sapienza, A. Vasanelli, R. Colombelli, C. Ciuti, Y. Chassagneux, C. Manquest, U. Gennser and C. Sirtori, Phys. Rev. Lett. **100**, 136806 (2008).

[45] S. De Liberato and C. Ciuti, Phys. Rev. Lett. **102**, 136403 (2009).

[46] A. K. Arora, E.-K. Suh, A. K. Ramdas, F. A. Chambers and A. L. Moretti, Phys. Rev. B **36**, 6142 (1987).

[47] M. A. Stroscio and M. Dutta, *Phonons in Nanostructures*, Cambridge University Press, (2001).

[48] D. E. Nikonov, A. Imamoğlu, L. V. Butov and H. Schmidt, Phys. Rev. Lett. **79**, 4633 (1997).

[49] S.-C. Lee and I. Galbraith, Phys. Rev. B **59**, 15796 (1999).

[50] S.-C. Lee and I. Galbraith, Phys. Rev. B **62**, 15327 (2000).

[51] P. Sotirelis, P. von Allmen and K. Hess, Phys. Rev. B **47**, 12744 (1993).

[52] J. J. Hopfield, Phys. Rev. **112**, 1555 (1958).

[53] P. Nataf and C. Ciuti, Nat. Comm. **1**, 72 (2010).

[54] Parameter for the III-V group were taken from: *www.ioffe.ru/SVA/NSM/Semicond*. For ZnSe we used data presented in: S. Adachi and T. Taguchi, Phys. Rev. B **43**, 9569 (1991). For CdTe we used instead: A. Manabe, A. Mitsuishi and H. Yoshinaga, Jpn. J. Appl. Phys. **6**, 593 (1967) and D. T. F. Marple, Phys. Rev. **129**, 2466 (1963).